

## MICROSTRUCTURAL AND SURFACE ANALYSIS OF Mg DOPED ZnO NANO PARTICLES SYNTHESIZED BY PRECIPITATION METHOD

S. SHANMUGAN<sup>a\*</sup>, K. NG JUN<sup>a</sup>, D. MUTHARASU<sup>a</sup>, I. A. RAZAK<sup>b</sup>

<sup>a</sup>*Nano Optoelectronics Research Laboratory, School of Physics, Universiti Sains Malaysia (USM), 11800, Minden, Pulau Pinang, Malaysia.*

<sup>b</sup>*X-ray Crystallography Laboratory, School of Physics, Universiti Sains Malaysia (USM), 11800, Minden, Pulau Pinang, Malaysia.*

Undoped and Mg doped ZnO nano particles were synthesized by wet chemical precipitation method and their optical and surface properties were characterized by Photoluminescence (PL), Raman spectra and Field Emission Scanning Electron Microscope (FESEM) respectively. Reduced structural and intrinsic defects such as zinc vacancies and oxygen interstitials was noticed with Mg doping and confirmed by PL spectra. The UV peak broadening and shifting to lower wavelength were evidenced the increased crystallite size or particle size and confirmed by Scanning Electron Microscope images. Higher Mg concentration in ZnO nano particles altered the band gap very close to the theoretical band gap of ZnO. Mg doped ZnO with higher concentration showed improved crystallinity by noticed with intense E<sub>1</sub>high mode than other concentrations. Mg doped ZnO nano particles were stress influenced and observed conversion from tensile to compressive with higher Mg concentration. SEM analysis showed the formation of flower and needle like nano structure of Mg doped ZnO nano particles. Overall the improved crystallinity and particles size was noticed with Mg doped ZnO nano particles.

(Received July 10, 2014; Accepted October 9, 2015)

*Keywords:* ZnO, Mg doping, Photoluminescence, Raman spectra, nano particles

### 1. Introduction

Nanotechnology have revolutionized many technology and industry sectors such as daily life materials, information technology, energy, environmental science, medicine, food safety, transportation, etc. Two major nanoscale effects are quantum confinement and very large surface area [1]. Correspondingly, physical properties such as electrical, thermal, optical and magnetic characteristics and chemical properties of nanoscale materials are size dependent and this offers the possibility for researchers to fine-tune a material property of interest to suite their application [2].

In material science, ZnO is classified as a II-VI semiconductor, with undoped ZnO is essentially a n-type semiconductor. Bulk ZnO have high mechanical and thermal stability, with modulus of hardness and melting point of 4-5 and 1975°C respectively. It also has fairly high thermal conductivity of about 1-1.2 Wcm<sup>-1</sup>K<sup>-1</sup> at room conditions [1]. Meanwhile, the specific heat capacity at constant pressure of ZnO is  $c_p=40.3$  Jmol<sup>-1</sup>K<sup>-1</sup>. However, thermal conductivity and specific heats at low temperature may vary significantly depending on the defects present [3]. ZnO is gifted with wide direct band gap (3.37 eV) and large exciton binding energy (60 meV). As the result, ZnO exhibit strong absorption and Photoluminescence in Ultra-Violet (UV) range therefore is transparent to visible light [4].

ZnO also has significant technological value particularly in electronic and technology industry. Moreover, crystal growth technology for ZnO is simpler, which results in potentially lower cost of ZnO based devices [5]. As the result, there are increasing number of reports on

---

\* Corresponding author: shagan77in@yahoo.co.in

researches and applications of ZnO in fabrications of optoelectronic devices such as Light Emitting Diode (LED), Laser diodes, photodetectors, photovoltaic cells [6], and Organic Light Emitting Diode (OLED) [7]. ZnO have brilliant future in transparent and flexible electronic applications [8]. Nanogenerators based on ZnO also become a new candidate for future green energy harvesting technology [9]. Moreover, Manganese doped ZnO is found to be a dilute magnetic semiconductors (DMS) which exhibit room temperature ferromagnetism. Based on the above, detailed study on the effect of metal doping on the ZnO nano structure is required and should be addressed their structural defect for tailoring the properties in selected application.

There are many methods are suggested for the synthesis of ZnO nano particles. Sol-gel [10], precipitation [11], hydrothermal [12], solvothermal [13], mechanochemical [14], spray pyrolysis [15], etc. are bottom-up process whereas the mechanical milling of ZnO powder method [16] is top-down process. Among these methods, the precipitation method, which is a wet chemical synthesis route, is relatively simple and low cost than the others [17]. In this study, undoped and Mg doped ZnO nano particles are synthesized by precipitation method and their surface and optical properties are evaluated. The observed data are reported and discussed here.

## 2. Experimental methodology

Mg doped ZnO nano particles were synthesized by precipitation method. AR grade Zinc Nitrate Hexahydrate  $Zn(NO_3)_2 \cdot 6H_2O$ , Sodium Hydroxide NaOH (Sigma Aldrich) and Magnesium Chloride Hexahydrate  $MgCl_2 \cdot 6H_2O$  (QREC) were used without further purification. For synthesis of pure ZnO, 29.749g of  $Zn(NO_3)_2 \cdot 6H_2O$  and 8.00g of NaOH were dissolved separately in 200ml of double distilled water to prepare 0.5M and 1.0 M solutions respectively. In all the literature, NaOH is added into zinc solution. Instead, the zinc solution is added into the NaOH solution which is to ensure the dissolution of zinc hydroxide precipitate into zinc complex ion and can serves as self-assembly units as well as providing an alkaline environment for reaction [18]. Consequently, NaOH solution was stirred by mechanical stirrer at 500 rpm and  $Zn(NO_3)_2 \cdot 6H_2O$  solution was added dropwise to it to form white precipitates. After the titration, the resulting solution was allowed to age for 2 hours. The precipitate was then filtered out, washed for 3-4 times with double distilled water and ethanol successively to remove unwanted solutions. Later, the precursor was dried in oven at 120°C for 4 hours and crushed into powder using ceramic mortar. The pure ZnO nanopowder was obtained. For Mg doping,  $MgCl_2 \cdot 6H_2O$  solution is added along with  $Zn(NO_3)_2 \cdot 6H_2O$  and prepared solution. In order to change the atomic concentration of Mg for doping to ZnO, the weight of  $MgCl_2 \cdot 6H_2O$  was varied and mixed with  $Zn(NO_3)_2 \cdot 6H_2O$  to achieve the doping concentration as mentioned in table – 1.

Table -1 Molar concentration of Mg in ZnO nano particles and sample name

Sample Name	Atomic Percentage (%mol) of $MgCl_2 \cdot 6H_2O$
0MZO	0 (pure ZnO)
2MZO	2
4MZO	4
6MZO	6
8MZO	8
10MZO	10

For easy understanding, the sample name, in which the front number represents the Mg doping percentage. For example, 2MZO represents 0.2 mole % Mg doped ZnO. Hereafter, the sample name is pronounced based on this nomenclature. The Raman spectrum of all samples was captured by using Horiba Jobin Yvon HR 800 UV Raman/Photoluminescence spectrometer with Argon laser source at 20mW as the excitation source. The 514.55 nm filter was inserted into the

system's optical compartment and the grating with 1800 grooves/mm was selected. The spectra was taken by the charge couple device which was peltier cooled at  $-77^{\circ}\text{C}$ , and hence intensity of the Raman scattered infrared was recorded with respect to their Raman shift in terms of wavenumber from  $200\text{-}800\text{ cm}^{-1}$ . Photoluminescence (PL) spectra for all samples were recorded by the using the same system as we used for Raman spectra but He-Cd laser source at  $20\text{mW}$  was used for illumination. In order to study the surface morphology, the FESEM images of undoped and Mg doped nano particles were captured and the surface properties are discussed.

### 3. Results and discussions

#### 3.1 Photoluminescence spectra analysis

Room temperature PL spectra of all samples were recorded as shown in fig. 1. Generally, from the PL spectra, there should be three main peaks such as a UV peak near band-edge emission around  $380\text{ nm}$ , a green emission peak around  $520\text{ nm}$  and an orange-red emission around  $600\text{ nm}$ . From the fig.2, it is clearly seen that there are two distinct peaks positions are identified from the undoped and Mg doped samples which are identified at around  $\sim 380\text{ nm}$  and  $\sim 550\text{ nm}$ . The small intensity peaks at  $\sim 380\text{ nm}$  are attributed to the effect of the free-exciton recombination.

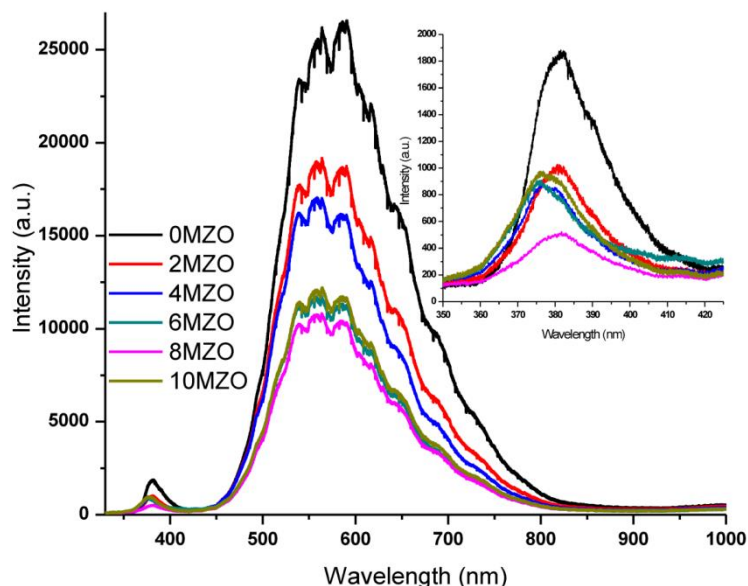


*Fig. 1 PL spectra of undoped and Mg doped ZnO nano particles. Inset fig: PL spectra observed between  $330\text{ nm}$  and  $450\text{ nm}$*

The broad peaks around  $\sim 550\text{ nm}$  state the structural defects and impurities in the structures. It is assigned as green emission peak and attributed to defects present in ZnO crystals, such as vacancies and interstitials of zinc and oxygen. The intensity of this peaks decreases with Mg concentration increases and might be related to the lower oxygen vacancies in the Mg doped samples. This green emission also involves transition from the band edge (or shallow level close to band) to a defect level.

It is also clearly seen that the intensities of PL peaks are decreasing as Mg concentration increasing. It refers that the structural defects are gradually decreasing as the Mg doping to ZnO lattice increasing. As observed the absence of broad orange-red emission from the PL spectra, the prepared samples are not having the oxygen interstitial defects [19]. Moreover, the characteristic peak of defects in ZnO ( $\sim 505\text{ nm}$ ) is not observed from our samples [20]. A broad deep level emission in the visible region near  $470\text{ nm}$  is ascribed for the structural defects and impurities in the system and not observed in our samples [21]. The intensity of deep level emission decreases as the Mg concentration increases and it is the evidence of reduced intrinsic defects such as zinc

vacancies and oxygen interstitials in the Mg doped samples. The observed results are contradicted to the published results [22] where the intensity of deep level emission was increased with Mg concentration.

According to the literatures [23,24], peaks related to a deep-level or trap-state emission located at 500 nm and 510 nm were not observed in our samples. From the fig. 1, the intensity of the exciton recombination related to the near-band edge emission decreases gradually with Mg concentration increases. Very low intensity was noticed with 8MZO samples. The intensity reduction is referred to the degradation of crystalline quality (see inset of fig.1). The peak broadening of PL spectra observed from the Mg doped samples is due to the strain developed in the doped samples. The FWHM value of UV emission increases with Mg concentration increases. It is attributed to the narrow size distribution of the nanoparticles in the prepared samples and agrees with the published results from different author [25]. The peak broadening of UV emission is also representing the decreased crystallinity with increased Mg concentration.

Moreover, the position of the near-band edge emission peaks of samples 4MZO, 6MZO and 10MZO are also shifting towards the left side (lower wavelength) and it is attributed to the effect of Mg doping in particle size and observed low intensity of the peak refers the increased particle size. The presence of the blue-shifting is remarkable because it suggests that the nanocrystals do not produce extra defects due to the introduction of the Mg ions [26]. Near band emission peaks tell us the bandgap of the prepared material and it is shifting towards low wavelength and approaches the theoretical energy band-gap of ZnO (3.37 eV). Especially, the samples named as 4MZO, 6MZO and 10MZO are very close to the band gap of ZnO. This blue shift of such peaks is attributed to the quantum confinement effects.

### 3.2 Raman spectra analysis

The microscopic nature of structural and morphological properties of nanocrystalline powder can be analyzed by using Raman spectra. Consequently, Raman spectra were recorded for all samples as shown in fig.2. it clearly shows that there are two distinct peak observed at  $\sim 367\text{ cm}^{-1}$  and  $\sim 439\text{ cm}^{-1}$  along with a broad peak at  $\sim 578\text{ cm}^{-1}$ .

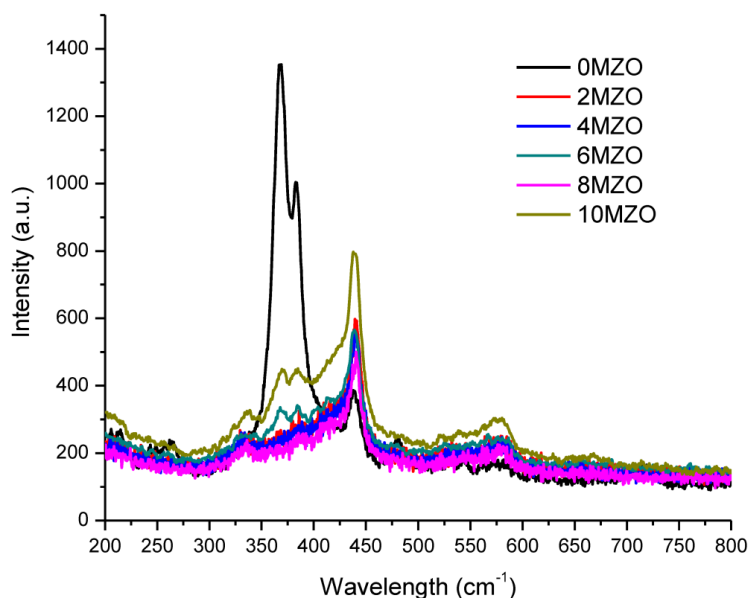


Fig.2. Raman Spectra of undoped and Mg doped ZnO nano particles

The peak observed at  $439\text{ cm}^{-1}$  corresponds to the  $E_2$  high mode of wurtzite ZnO. The peak at  $\sim 578\text{ cm}^{-1}$  is assigned to the  $E_1$  (LO) mode of ZnO quantum dots and the peak intensity is enhanced and shifted to lower wavenumber due to a resonance at the excitation wavelength and the presence of impurity (Mg) induced scattering [27]. The strong peak at  $\sim 382\text{ cm}^{-1}$  are assigned to

$A_1(\text{TO})$  mode of hexagonal ZnO and their intensity decreases noticeable for Mg doped ZnO. A small peak at  $\sim 332$  and  $\sim 380 \text{ cm}^{-1}$  are also noticed with the Mg doped ZnO nano particles and assigned the second order ( $E_2$  (high) –  $E_2$  (low)) and  $A_1$  (TO), respectively [28]. The same observation was noticed for Cu doping in other work [29]. The second order ( $E_2$  (high) –  $E_2$  (low)) peaks are not observed with undoped ZnO particles but a peak located at  $\sim 382 \text{ cm}^{-1}$  are observed as shoulder peak for the undoped ZnO nanoparticles and it is assigned to  $A_1$  (TO) modes.

The presence of highly intense  $E_2$  high band is the indication of highly crystalline nature of Wurtzite ZnO nanostructure. From the fig. 2, it is clearly seen that the crystalline nature of the ZnO increases with Mg doping concentration increases. High value of the peak intensity is noticed with 10MZO sample than other samples. There is no peak shifting for  $\sim 332 \text{ cm}^{-1}$  emission. The increase in peak intensity was also noticed with Cu doping in other research work [30]. For 10MZO sample, a small intensity peaks are observed at  $\sim 539$  &  $\sim 578 \text{ cm}^{-1}$  and assigned to  $A_1$  (LO) and  $E_1$  (LO) modes respectively. The presence of these two modes are attributed to the random orientation of ZnO [31] and also assigned to surface optical modes predicted theoretically and O vacancies,  $Zn_i$  or combination of the two[32].

The  $E_2$  high mode shift towards higher frequency for 8MZO sample and attributed to the effect of stress developed in the ZnO lattice. Generally, shift of  $E_2$  phonon frequency is considered as a stress deciding factor from the Raman spectra. An increase in the  $E_2$  phonon frequency is ascribed to compressive stress, whereas a decrease in the  $E_2$  phonon frequency is ascribed to tensile stress. This is because of the lattice mismatch and distortion in the crystal lattice. It can be altered by introducing a dopant to the lattice and cause the lattice distortion in the crystal which is usually different from the atomic radii of different elements [33]. Based on this assessment, it is concluded that the 8MZO sample is under compressive stress i.e., a conversion from tensile to compressive was occurred as with Mg concentration increases in the ZnO.

### 3.3 Surface morphology analysis

The recorded surface morphology of all samples is displayed in fig.3. It clearly reveals the change in surface properties of doped ZnO nano particles. An interesting surface morphology was notice with all Mg doped samples.

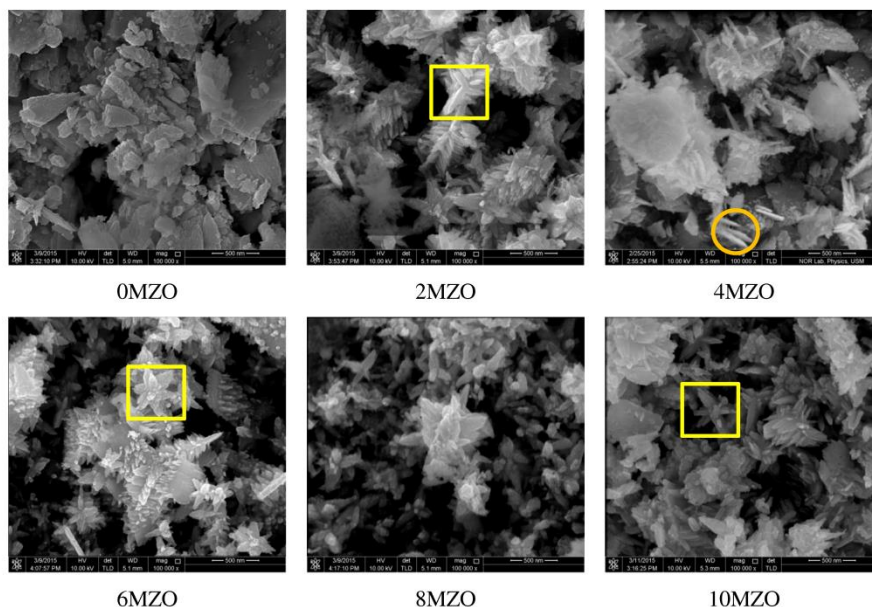


Fig.3 FESEM images of undoped and Mg doped ZnO nano particles

From the fig.3, it is observed that a flower type nano structure (yellow square) is noticed with all Mg doped samples especially for 2MZO, 6MZO, 10MZO samples. Undoped sample shows the big grain with agglomeration. It can be seen from the fig.3, that the particle are needle

like structure and their thickness or diameter increases with Mg concentration increases. Grain agglomeration is noticed clearly with 4MZO samples and it clearly indicates the needle like structure (orange circle). Fig.3 also shows the increased particle size with Mg concentration increases. Highly dense particles are noticed with 10MZO samples with needle like crystal structure. It is also noticed from the fig.3 that the nano structure growth is in particular direction and the nano crystal is acting as seed crystal for further growth.

#### 4. Conclusion

Mg doped ZnO nano particles were synthesized by Wet chemical route and analyzed by PL and Raman spectra. PL spectra was evidenced the formation of high crystalline ZnO nano particles with reduced structural defects for Mg doping. The particle size improvement for Mg doped ZnO was noticed by SEM analysis and proved by UV emission from PL spectra. The band gap tuning close to theoretical value was demonstrated by Raman spectra. Flower and needle like nano structure of Mg doped ZnO were confirmed by SEM analysis.

#### Acknowledgements

The authors express their gratitude for the FRGS project (203/PFIZIK/6711350) that provides the fund to carry out the research work successfully in school of physics. In addition, the authors would like to acknowledge for the use of research facilities such as FESEM, PL and Raman spectroscopy etc., available in NOR Lab, School of Physics, Universiti Sains Malaysia.

#### References

- [1] L.L. Yang, Q.X. Zhao and Magnus Willander, *Journal of Alloys and Compounds*, **469** 623, (2009).
- [2] Nano.gov., (2015). *What It Is and How It Works / Nano*. Retrieved 14 March 2015, from <http://www.nano.gov/nanotech-101/what>
- [3] C. Jagadish and S. Pearton, Elsevier, 1, (2006).
- [4] G.C. Yi, C. Wang and W. Il Park, *Semiconductor Science and Technology*, **20**, 22 (2005)
- [5] Ü. Özgür, Ya. I. Alivov, C. Liu, A. Teke, M. A. Reshchikov, S. Doğan, V. Avrutin, S.-J. Cho, H. Morkoç, *Journal of Applied Physics*, **98**, 041301 (2005)
- [6] A.B. Djurišić, A.M.C. Ng, X.Y. Chen, *Progress in Quantum Electronics*, **34**, 191 (2010)
- [7] M. Belhaj, C. Dridi, H. Elhouichet, *Journal of Luminescence*, **157**, 53 (2015)
- [8] A. Mofor, A. Bakin, B. Postels, M. Suleiman, A. Elshaer and A. Waag, *Thin Solid Films*, **516**, 1401 (2008)
- [9] N.I. Jun, J.D. Yong, L. Sunwoo, K.S. Hyun, C.J. Woo and S.P. Kyun, *Microelectronic Engineering*, **110**, 282 (2013)
- [10] K. Omri, I. Najeh, R. Dhahri, J. El Ghoul, and L. El Mir. *Microelectronic Engineering* **128**, 53 (2014)
- [11] D. Raoufi, *Renewable Energy*, **50**, 932 (2013)
- [12] S. Kumar and P. Sahare, *Optics Communications*, **285**, 5210 (2012)
- [13] C. Yanfeng, Z. Chaojie, H. Weixin, S. Yue, and H. Hong, *Materials Letters*, **141**, 294 (2015)
- [14] A. K. -Radzimska and T. Jesionowski, *Materials*, **7(4)**, 2833 (2014)
- [15] H.R. Ghaffarian, M. Saiedi and M.A. Sayyadnejad, *Iranian Journal of Chemistry and Chemical Engineering*, **30**, 1 (2011)
- [16] S. Suwanboon and P. Amornpitoksuk, *Procedia Engineering*, **32**, 821 (2012)
- [17] A. Moharram, S. Mansour, M. Hussein and M. Rashad, *Journal of Nanomaterials*, **2014**, 1 (2014)
- [18] S.S. Alias, A.B. Ismail and A. A. Mohamad, *Journal of Alloys And Compounds*, **499**, 231 (2010)

- [19] P. Uthirakumar, B. Karunagaran, S. Nagarajan, E.K. Suh and C.H. Hong, *Journal of Crystal Growth*, **304**, 150 (2007)
- [20] H. Chun, T. Sasaki, Y. Shimizu and N. Koshizaki, *Applied Surface Science*, **254**, 2196 (2008)
- [21] F. Gu, S.F. Wang, M.K. Lii, G.J. Zhou, D. Xu and D.R. Yuan, *Journal Physics and Chemistry. B*, **108**, 8119 (2004).
- [22] M. Arshad, M.M. Ansari, A.S. Ahmed, P. Tripathi, S.S.Z. Ashraf, A.H. Naqvi and A. Azam, *Journal of Luminescence*, **161**, 275 (2015)
- [23] C.S. Lin, C.C. Hwang, W.H. Lee and W.Y. Tong, *Material Science Engineering B*, **140**, 31 (2007)
- [24] K. Vanheusden, W.L. Warren, C.H. Seager, D.R. Tallant, J.A. Voigt, B.E. Gnade, *Journal of Applied Physics*, **79**, 7983 (2007)
- [25] A.N. Mallika, A. R. Reddy, K.S. Babu, Ch. Sujatha and K.V. Reddy, *Optical material*, **36**, 879 (2014)
- [26] Y. S. Wang, P. J. Thomas, and P. O'Brien, *Journal Physics and Chemistry. B*, **110**, 21412 (2006).
- [27] G. Shuxia, D. Zuliang and D. Shuxi, *Physica Status Solidi B*, **246**, 2329 (2009)
- [28] J. Serrano, A.H. Romero, F.J. Manjón, R. Lauck, M. Cardona and A. Rubio, *Physical Review. B*, **69**, 094306 (2004),.
- [29] P. D. Sahare and Vipin Kumar, *International Journal of Innovative Technology and Exploring Engineering (IJITEE)*, **3**, 15 (2013),
- [30] B. Yang, A. Kumar, P. Feng and R. S. Katiyar, *Applied Physics Letters*, **92**, 233112 (2008).
- [31] B. Cao, W. Cai, H. Zeng and G. Duan, *Journal of Applied Physics*, **99**, 073516 (2006)
- [32] S. Baskoutas, P. Giabouranis, S.N. Yannopoulos and V. Dracopoulos, *Thin Solid Films*, **515**, 8461 (2007)
- [33] L.S. Shou, D. Huang, C.H. Tu, C.H. Hou and C.C. Chen, *J. Phys. D: Applied Physics Letters*, **42**, 095420 (2009).